

# Regularising the JNW and JMN naked singularities

Kunal Pal,<sup>1,\*</sup> Kuntal Pal,<sup>1,†</sup> Pratim Roy,<sup>2,3,‡</sup> and Tapobrata Sarkar<sup>1,§</sup>

<sup>1</sup>*Department of Physics, Indian Institute of Technology Kanpur,  
Kanpur 208016, India*

<sup>2</sup>*Harish-Chandra Research Institute, Chhatnag Road, Jhansi, Prayagraj 211019, India*

<sup>3</sup>*Homi Bhabha National Institute, Training School Complex, Anushaktinagar, Mumbai 400094, India*

We extend the method of Simpson and Visser (SV) of regularising a black hole spacetime, to cases where the initial metric represents a globally naked singularity. We choose two particular geometries, the Janis-Newman-Winicour (JNW) metric representing the solution of an Einstein-scalar field system, and the Joshi-Malafarina-Narayan (JMN) metric that represents the asymptotic equilibrium configuration of a collapsing star supported by tangential pressures as the starting configuration. We illustrate several novel features for the modified versions of the JNW and JMN spacetimes. In particular we show that, depending on the values of the parameters involved, the modified JNW metric may represent either a two way traversable wormhole, or it may remain the original naked singularity. On the other hand, the SV modified JMN geometry is always a wormhole. Particle motion and observational aspects of these new geometries are investigated and are shown to possess interesting features.

arXiv:2206.11764v1 [gr-qc] 23 Jun 2022

---

\* [kunalpal@iitk.ac.in](mailto:kunalpal@iitk.ac.in)

† [kuntal@iitk.ac.in](mailto:kuntal@iitk.ac.in)

‡ [pratimroy@hri.res.in](mailto:pratimroy@hri.res.in)

§ [tapo@iitk.ac.in](mailto:tapo@iitk.ac.in)

## I. INTRODUCTION

Despite being the most successful theory of gravity till date, it is widely believed that general relativity (GR) [1] may break down in high curvature regimes, where it will be replaced by an yet unknown theory of quantum gravity. For this reason, the final fate of a gravitational collapse, starting from some well behaved set of initial data is still an open problem, as the analysis carried out in the classical (or effectively semiclassical) theory may received important quantum corrections in the strong gravity regime. In this context, two important questions are known to arise. First, if the regular interior of a collapsing star in realistic situations produce a spacetime singularity, which is specified by a diverging curvature scalar, and secondly, whether this singularity is visible to an asymptotic observer. The latter is thought to be prohibited by the cosmic censorship conjecture (CCC) of Penrose [2], which is yet to be proved in full generality. In the absence of a fully accepted theory of quantum gravity, a popular line of research to study the above mentioned problems is to construct a model of ‘regular black holes,’ where the singularity is replaced by a region of regular curvature. On the other hand, the notion of a ‘horizonless compact object’ with or without a singularity, like a wormhole (WH) [3, 4], a naked singularity (NS) etc., has also gained considerable attention in the literature. Though the presence of a NS without an event horizon would violate the CCC, there are well studied models in the literature, where the end states of a viable collapse process produces a NS, and therefore it is fair to say that a firm conclusion is yet to be reached in the matter.

Starting from the seminal work of Bardeen [5], there are abundant models of regular black holes which are constructed either from a purely phenomenological point of view, or as solutions of an effective semiclassical gravity theory (for a review and further references, see [6]). The basic idea of these kinds of phenomenological models is to replace the Schwarzschild mass by some general family of mass functions, that would render the curvature scalars finite everywhere in the spacetime. Though this looks promising at first sight, there are many models of regular black holes that have an inner Cauchy horizon, and its instability under mass inflation can be problematic for realistic model building (see [7] and references therein). In view of the above discussions, an interesting one parameter model for regularising the Schwarzschild singularity was proposed recently by Simpson and Visser (SV) [8], where the central singularity was replaced by a regular region, that can be timelike, null, or spacelike, depending on the parameter involved in the geometry, and the global geometry represents either a traversable WH or a regular BH with one horizon. Such models, dubbed as ‘black-bounce’ spacetimes, not only resolve the Schwarzschild singularity, but also provide a link between two different classes of spacetime structures, namely the BH and the WH, and therefore is a promising way of further constructing regular black holes and resolving the singularity problem of classical GR. See, [10] - [14] for a selection of recent works in this direction.

In this paper, we extend the method of SV and construct regular solutions starting from a globally naked singularity, and in the process unify two different classes of metrics, namely the WH and NS. To this end, we first apply the SV regularisation scheme to the Janis-Newman-Winicour [15, 16] class of spacetimes which have a naked curvature singularity at a finite radial location, and reduces to the Schwarzschild black hole for a particular limit of the parameters involved. We construct a deformed JNW metric that interpolates between a BH, WH and NS for

different ranges of the parameters. As a second example, we construct a similar deformation of the Joshi-Malafarina-Narayan [17] spacetime, that contains a central NS and is known to be a result of gravitational collapse of regular initial data. In the rest of this paper, we discuss the resulting metrics and show that these are indeed rich in terms of global spacetime structures and observational aspects. We always work in units where the gravitational constant and the speed of light are set to unity.

## II. DEFORMED JANIS-NEWMAN-WINICOUR SOLUTION

The Janis-Newman-Winicour metric [15, 16] is a static, spherically symmetric solution of the Einstein field equations in the presence of a minimally coupled scalar field, and is given by the line element

$$ds^2 = -\left(1 - \frac{b}{r}\right)^\gamma dt^2 + \left(1 - \frac{b}{r}\right)^{-\gamma} dr^2 + \left(1 - \frac{b}{r}\right)^{1-\gamma} r^2 d\Omega^2 . \quad (1)$$

The parameters  $\gamma$  and  $b$  appearing in the JNW metric are related to the ADM mass  $M$  and the scalar charge  $q$  by the relations

$$\gamma = \frac{2M}{b} , \quad b = 2\sqrt{M^2 + q^2} . \quad (2)$$

In the limit of vanishing scalar charge  $q \rightarrow 0$ , the JNW solution reduces to the Schwarzschild black hole. In the general case, with  $q \neq 0$ , and real, it can be seen from Eq. (2) that  $\gamma < 1$ . This fact also indicates that the JNW metric is only valid up to the coordinate location  $r = b$ . It can also be checked that for  $\gamma < 1$ , this metric has a curvature singularity at  $r = b$ , and since the metric does not possess any event horizon, it is a naked singularity [18]. On the other hand, when the scalar charge  $q$  is imaginary such that  $\gamma > 1$ , this metric represents a symmetric traversable WH with two asymptotically flat regions [19, 20].

Now we apply the SV method via the replacement  $r \rightarrow \sqrt{r^2 + c^2}$ , without modifying the form  $dr$  (in which case it will simply be an uninteresting overall coordinate transformation) in the JNW solution, and the resulting metric becomes

$$ds^2 = -\left(1 - \frac{b}{\sqrt{r^2 + c^2}}\right)^\gamma dt^2 + \left(1 - \frac{b}{\sqrt{r^2 + c^2}}\right)^{-\gamma} dr^2 + \left(1 - \frac{b}{\sqrt{r^2 + c^2}}\right)^{1-\gamma} (r^2 + c^2) d\Omega^2 . \quad (3)$$

Here  $c$  (not to be confused with the speed of light), the SV parameter, is a real and positive quantity having dimensions of length. The range of coordinates, other than that of  $r$  are same as before, and the range of  $r$  depends upon the relative values of  $c$  and  $b$ , as we explain below in detail. Also, it can readily be seen that the original symmetries and the asymptotic properties of the JNW metric are preserved with the new one. We will get back the JNW metric in the limit  $c \rightarrow 0$  and the SV metric (i.e., the deformed Schwarzschild metric) in the limit  $\gamma \rightarrow 1$ .

Now we elaborate upon the metric of Eq. (3) (which we shall call the SV-JNW solution from now on) for different parameter ranges. For this, it will be useful to define a coordinate transformation  $k^2 = r^2 + c^2$ , doing which we get

$$ds^2 = -\left(1 - \frac{b}{k}\right)^\gamma dt^2 + \left(1 - \frac{b}{k}\right)^{-\gamma} \frac{k^2}{k^2 - c^2} dk^2 + \left(1 - \frac{b}{k}\right)^{1-\gamma} k^2 d\Omega^2 . \quad (4)$$

To gain more insight into the structure of the metric, we use another coordinate transformation

$$R^2 = \left(1 - \frac{b}{k}\right)^{1-\gamma} k^2, \quad (5)$$

after which the final form of the metric is,

$$ds^2 = -\left(1 - \frac{b}{k(R)}\right)^\gamma dt^2 + \left(1 - \frac{b}{k(R)}\right)^{-\gamma} \frac{k(R)^2}{k(R)^2 - c^2} \left(\frac{1}{D(k)^2 \left(1 + \frac{b(1-\gamma)}{2(k-b)}\right)^2}\right) dR^2 + R^2 d\Omega^2, \quad (6)$$

and we have defined  $D(k) = \left(1 - \frac{b}{k}\right)^{\frac{1-\gamma}{2}}$ . Since Eq. (5) can be inverted in principle to obtain  $k$  in terms of the new variable  $R$ , we have retained its implicit dependence. To gain insights into this metric we now compare this to the canonical Morris-Thorne WH [21]

$$ds^2 = -\exp(2\Phi)dt^2 + \frac{1}{1 - \frac{B(R)}{R}} dR^2 + R^2 d\Omega^2, \quad (7)$$

where  $B(R)$  is the shape function and  $\Phi(R)$  is the redshift function. For our metric the shape function is given by

$$B(k(R)) = k \left[ 1 - \left(1 - \frac{b}{k}\right)^\gamma \left(1 - \frac{c^2}{k^2}\right) D^2 \left(1 + \frac{b(1-\gamma)}{2(k-b)}\right) \right]. \quad (8)$$

The  $g_{RR}$  component of the above metric has three zeros, respectively at  $k_1 = b$ ,  $k_2 = c$ , and  $k_3 = \frac{b}{2}(\gamma+1)$ . Similarly from the form of the redshift function, we can see that the solution contains a singularity at  $k_1 = b$ . So, depending upon the nature of the parameters involved, we can have several interesting cases here, which we now detail. First we shall consider the cases with  $\gamma < 1$ .

- $\gamma < 1$  and  $b < c$  : Here,  $k_3 < k_1$  and hence the root  $k_3$  does not play any significant role, since the metric is not valid upto the radial value corresponding to  $k_3$ . In this case, it can readily be seen that the original domain of validity of the JNW metric (up to  $r \geq b$ ) has changed, and the metric can be continued from  $r = \infty$  to  $r = -\infty$ , through  $r = 0$ . The metric then represents a traversable wormhole, with a timelike throat at  $r = 0$ , connecting two asymptotically flat regions. This is very different from the usual JNW solution, where no WH branch exists for  $\gamma < 1$ . For completeness, we explicitly checked that the conditions for a traversable wormhole [3] are satisfied here :
  - Absence of horizons - This can be seen from the metric written in Eq. (4), from which it is evident that the spacetime does not contain any horizon as long as  $b < c$  is satisfied.

- Flaring out condition - This condition satisfied by a traversable wormhole embodies the fact that the throat is the location of minimum area (see [22] for a detailed discussion). Mathematically, the flaring out condition implies that  $A'(r = r_0) = 0, A''(r = r_0) > 0$ , where the prime denotes a derivative with respect to the radial coordinate. For the metric of Eq. (3), we note that the area of the two sphere is  $A(r) = \left(1 - \frac{b}{\sqrt{r^2 + c^2}}\right)^{1-\gamma} (r^2 + c^2)$ , and hence  $A'(r = r_0) = 0 \implies r_0 = 0$ , i.e., we have a stationary point of the area of the spherical surface at the throat  $r = r_0 = 0$ . To check that this represents a minimum we only need to note that  $A''(r = r_0) = \frac{2(2c-b(1+\gamma))}{c(1-\frac{b}{c})^\gamma}$ . Thus as long as the condition  $b < c$  satisfied  $A''(r = r_0) > 0$ , and we see that the area is indeed minimum at the location of the throat, and that the flaring out condition is indeed satisfied.

(iii) Non-singular nature - To show that the resulting geometry is non singular everywhere - which is required for the metric to represent a wormhole geometry, we calculate the curvature scalars. The Ricci scalar in this case  $R \sim (1 - \frac{b}{\sqrt{r^2+c^2}})^{-2}$ , from where we see that it is indeed finite everywhere, including  $r = 0$  and  $r = b$ . Similarly, the Kretschmann scalar  $K \sim (1 - \frac{b}{\sqrt{r^2+c^2}})^{-4}$  which is also finite everywhere.

- $\gamma < 1$  and  $b > c$  : Here, the range of the radial coordinate is restricted to  $\sqrt{b^2 - c^2} < r < \infty$ , a condition analogous to that in the original JNW metric. The Ricci scalar  $R \sim (1 - \frac{b}{\sqrt{r^2+c^2}})^{-2}$ , and diverges in the limit  $r \rightarrow \sqrt{b^2 - c^2}$  (the same conclusion can be shown to be valid for the Kretschmann scalar curvature). On the other hand, from the form of the metric, it can be seen that there is an event horizon precisely at the location of the curvature singularity. So, as in the case of the original JNW metric [18], we conclude that the singularity is not covered by that of an event horizon from a distant observer, and that the spacetime represents a naked singularity for the above parameter ranges.

- $\gamma < 1$  and  $b = c$  : This is the limiting case of the two earlier ones. As explained above, here the metric consists of a throat (minimum of the local area), an event horizon, and the curvature singularity, all at the location  $r = 0$ . So the metric represents a one way wormhole with a singular throat.

Now we examine the solutions for the range  $\gamma > 1$ . This case is similar to that of the original JNW WH [19, 20], although due to the introduction of the parameter  $c$ , we will have a richer geometric structure. First note that here  $k_3 > k_1$ , and in the original coordinate  $r$ , the three zeros are written as

$$r_1 = \sqrt{b^2 - c^2}, r_2 = 0, r_3 = \sqrt{\frac{b^2}{4}(\gamma + 1)^2 - c^2} . \quad (9)$$

As before we will consider two cases  $b > c$  and  $b < c$  and their limiting cases.

- $b < \frac{b}{2}(\gamma + 1) < c$  : Here, we consider only the valid root of Eq. (9) which is real. Again we see that the region of validity of the metric is increased from  $r = -\infty$  to  $r = \infty$ . In this case, the metric represents a traversable wormhole with a throat at  $r = 0$ . Again, one can check the validity of the WH features here, but we omit the details for brevity.

- $b < c < \frac{b}{2}(\gamma + 1)$  : In this case, the value of  $\gamma$  is such that the third root of Eq. (9) is real. We can immediately see that this metric represents a traversable WH with a throat at  $r_3$ , with similar arguments as before.

Finally note that there is no possibility of any NS branch here, as even in the case  $c < b < \frac{b}{2}(\gamma + 1)$ , the metric represents a WH, since the metric is still valid upto  $r_3$ . So we can conclude that the NS is fully regularised here, following the SV method.

### A. Photon motion in SV-JNW background

Now we discuss the motion of a photon in the SV-JNW background, and the resulting shadow structure of the metric in Eq. (3). Since the metric is spherically symmetric, the structure of the null geodesics is fairly simple, and here our main goal will be to compare and contrast this spacetime with its two limits, namely the SV metric ( $\gamma \rightarrow 1$ ) and the JNW metric ( $c \rightarrow 0$ ) in terms of the effective potential encountered by a photon moving in these

three spacetimes.<sup>1</sup> The standard approach to study the null geodesics motion and consequently finding the photon sphere, which are the unstable orbits of light rays, is to use the Hamilton-Jacobi equation. After performing a standard analysis, the effective potential encountered by a photon in a spherically symmetric background can be written as [24]

$$V_{eff}(r) = g_{tt} \frac{C + L^2}{\mathcal{B}(r)}, \quad (10)$$

where  $g_{tt}$  represents the temporal component of the metric and  $\mathcal{B}(r)$  is its two sphere part. Here,  $C$  and  $L$  are the Carter's constant and the angular momentum respectively, and both of them are conserved quantities associated with the photon motion. Using the relevant functions from Eq. (3), we get the expression of the effective potential for the photon motion to be

$$V_{eff}(r) = \frac{C + L^2}{r^2 + c^2} \left( 1 - \frac{b}{\sqrt{r^2 + c^2}} \right)^{2\gamma-1}. \quad (11)$$

Now, circular photon orbits can be obtained by imposing the condition of vanishing radial velocity along with the condition for the extremum of the effective potential,  $\dot{r} = 0$  and  $V'_{eff} = 0$ . Typically this extremum turns out to be a maximum, and photon orbits are unstable. Solving this constraint, we obtain the following three solutions,

$$r_1 = 0, \quad r_2 = \sqrt{b^2 - c^2}, \quad \text{and} \quad r_3 = \left\{ b^2 \left( \frac{1}{4}(2\gamma - 1)^2 + (2\gamma - 1) + 1 \right) - c^2 \right\}^{1/2} = \sqrt{b^2 \left( \gamma + \frac{1}{2} \right)^2 - c^2}. \quad (12)$$

This gives correct result for SV metric ( $\gamma \rightarrow 1$ ) [8] and in the limit  $c \rightarrow 0$ , it correctly reduces to the known photon sphere of the JNW metric. Now, depending on the range of the various parameters ( $b, c, \gamma$ ), the above three roots give the photon sphere in the spacetime, and we will now discuss them. In this section we shall consider only values of  $\gamma < 1$ .

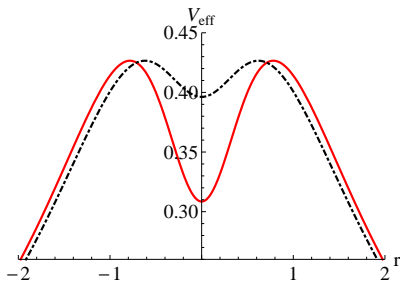


FIG. 1.  $V_{eff}$  for the WH branch when  $c > b$ . The solid red curve represents the case with  $c = 1.1$ , and the dotted black is with  $c = 1.2$ . For both,  $b = 1, \gamma = 0.85, C = L = 1$ .

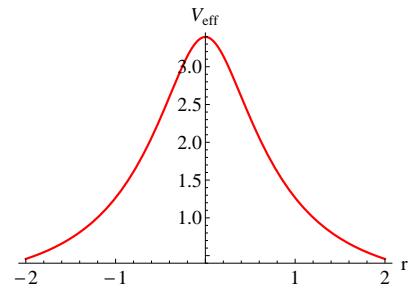


FIG. 2. Plot of the effective potential for the WH case. The solid red curve represents the case with  $\gamma = 0.35$  for which maximum of  $V_{eff}(r)$  is at  $r_1$ . We have set  $b = 1, c = 1.1, C = L = 1$ .

- Photon motion for  $b < c$  : As we have discussed above, in this case the spacetime is a wormhole (WH) with a throat at  $r = 0$ . We can directly see from Eq. (12) that in this case, the solution  $r_2$  is not real, and the parameter

<sup>1</sup> The observational features of the above two cases are well studied in the literature for example see [8] for SV metric and [23, 24] for the JNW metric.

range the other two solutions might be relevant here. In this context, we note that the motion of light in wormhole backgrounds has been widely studied in the literature, see, e.g., [25] and references therein. Here the stand out feature for the wormhole background is the fact that apart from the conventional photon sphere outside the throat, the throat can itself work as a location of the photon sphere (i.e., a location of the maximum of the effective potential), see [26] for details. For our purposes, the two sub-cases are important in this class of solutions, namely whether the third root  $r_3$  is real or not corresponding to some given parameter range.

First, we consider the case when  $r_3$  is real. Then the root  $r_3$  ( $> r_1$ ) can be real only if  $\gamma > \frac{1}{2}$ . This range of gamma  $\frac{1}{2} < \gamma < 1$  is the same as that of the JNW metric, and when this condition is satisfied,  $r_3$  is a location of photon sphere. The plot of the effective potential is shown in fig. 1, for two different values of  $c$  with fixed  $\gamma = 0.85, b = 1$ . A light ray from our universe will encounter this photon sphere first and will form shadow [27]. Now the interesting case happens if we continue to increase  $c$ , such that the value of  $r_3$  saturates.

Next, consider the case where  $r_3$  not real, which can be due to two different reasons. Firstly if  $\gamma < 1/2$ , then  $r_3$  is not physical for any value of  $b, c$  (with  $b < c$ ). In this case, the throat at  $r_1$  acts as the location of the unstable orbits of photon and generates the shadow. We note that this is in contrast to JNW spacetime, where no photon sphere is possible for  $\gamma < 0.5$ . This case is illustrated in fig. 2.

On the other hand even if  $\gamma > 1/2$ , since  $\gamma$  is always less than unity, there is an upper bound on  $c$  for which  $r_3$  can be real. This can be found from setting  $\gamma = 1$  in  $r_3$ , from which we conclude that if  $c > \frac{3b}{2}$ , then  $r_3$  is not real, and in this case also  $r_1$  acts as a location of unstable photon orbit, see the plot of the effective potential in Fig. 3.

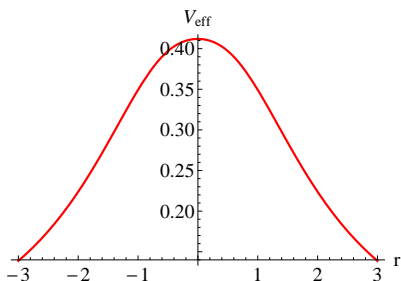


FIG. 3.  $V_{eff}$  for the WH case. The curve represents the case with  $\gamma = 0.85$  for which maximum of  $V_{eff}(r)$  is at  $r_1$ . Here,  $b = 1, c = 1.5, C = L = 1$ .

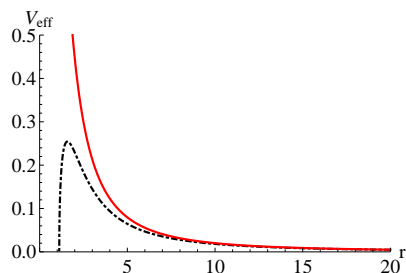


FIG. 4.  $V_{eff}$  for the NS case. The solid red curve is with  $\gamma = 0.45$ , and the dashed black curve is for  $\gamma = 0.85$ . For both plots,  $b = 1.5, c = C = L = 1$ .

- Photon motion for  $b > c$  : In this case, the spacetime itself is valid upto a radial distance  $r = \sqrt{b^2 - c^2}$ , and it represents a naked singularity at that coordinate location. Now clearly, among the three solutions in Eq. (12), the  $r_1 = 0$  solution is not relevant here, and since the second solution  $r_2 = \sqrt{b^2 - c^2}$  is the location of the curvature singularity itself, it cannot be the physically relevant photon sphere. Importantly however, depending on the range of  $\gamma$ , the solution  $r_2$  decides whether the third solution gives rise to a physically relevant photon sphere or not, since if for some value of  $\gamma$ , it turns out that  $r_3 < r_2$ , then  $r_3$  is not physical, even if it a real solution.

The allowed range of  $\gamma$  can be found from Eq. (12) as  $\gamma > \frac{1}{2}$ , as we are considering the case  $b > c$ . So in this case, the spacetime has **one photon sphere** at the coordinate location  $r_3$  for  $\frac{1}{2} < \gamma < 1$  and **no photon sphere**

for  $0 < \gamma < \frac{1}{2}$ . Note that as long as  $\gamma > \frac{1}{2}$ , there is no restriction on the values of  $b, c$  except  $b > c$ , unlike above case, as  $r_3$  will always be real as long as above conditions are satisfied. In Fig. 4, we have shown the effective potential in this case.

Note that unlike the WH case, here we cannot have a photon sphere for  $\gamma < 0.5$ , as  $r_3 < r_2$  will always be satisfied, and we will have a NS configuration without a photon sphere. In this way the NS branch mimics the behaviour of photons in the JNW metric.

To summarize, the SV-JNW spacetime we have constructed can have one photon sphere (at  $r_3$  or  $r_1$ ) or can have no photon sphere at all, depending on the relative values of the parameters  $b$  and  $c$ , as well as that of  $\gamma$ . This behaviour is to be contrasted with the standard JNW metric and the SV metric, which are two particular limits of our metric. To this end, a qualitative comparison of the effective potentials encountered by a massless particles moving in SV, JNW and SV-JNW solutions is given in fig 5 (for the SV and SV-JNW solutions, only the WH branches are plotted). In particular, note the contrast between the JNW and SV-JNW cases. Due to the fact that the SV-JNW solution has a WH branch, its effective potential continues into the other universe also. The large  $r > 0$  behaviours of all these cases are similar, since all of them are asymptotically Minkowski spacetimes.

## B. Energy conditions

In this subsection, we shall analyze the energy conditions corresponding to the metric in Eq. (3). Since most of the wormhole spacetimes discussed in the literature violate the energy conditions, it is important to check this out for our metric as well.

The EM tensor can be calculated from the Einstein equations  $G_{\mu\nu} = T_{\mu\nu}$ . Since our considered geometry does not possess any event horizon, the components of the energy momentum tensor, given by  $\rho = -T_t^t, p_r = T_r^r, p_\theta = T_\theta^\theta = T_\phi^\phi$  are valid for all values of the coordinate  $r$  for which the metric is valid i.e., for the WH branch the range is  $-\infty < r < \infty$ , and given for the NS branch by  $\sqrt{b^2 - c^2} \leq r < \infty$ . It is enough to check if the null energy condition (NEC) is violated because if that is the case, then all the other energy conditions are violated as well. The NEC in this case is given from  $\rho + p_r \geq 0$  and  $\rho + p_\theta \geq 0$ . Before proceeding, we recall that NEC is violated for SV spacetimes in every parameter range, whereas the JNW metric satisfies the NEC everywhere.

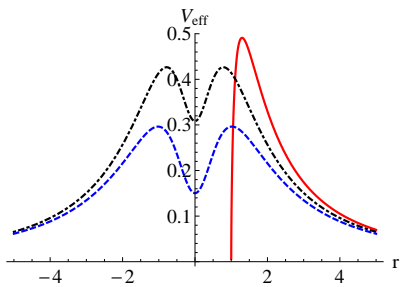


FIG. 5. Effective potentials encountered by a massless particle for the SV (blue dashed curve), JNW (red curve) and SV-JNW (black dot-dashed curve) spacetimes.

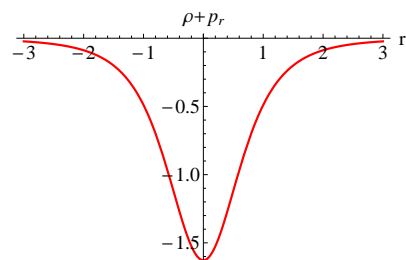


FIG. 6.  $\rho + p_r$  for the WH branch with  $\gamma = 0.45, c = 1.1, b = 0.1$ . The NEC is always violated.



In Figures 6 and 7, we have plotted  $\rho + p_r$  for both the WH and NS branch of the metric of Eq. (3), with the parameters indicated in the respective captions. As can be seen, the WH branch violates the NEC everywhere, while for the NS branch, by decreasing the value of  $\gamma$ , this condition can be satisfied for all values of  $r$ . In this case only we need to check the second condition also. In Fig. 8, we have plotted the quantity  $\rho + p_\theta$  for the same parameter values as in Fig. 7, and as can be seen, the plot with  $\gamma = 0.25$  satisfies the condition  $\rho + p_\theta > 0$  as well. Thus we conclude that, in contrast with the SV solution, for sufficiently small values of  $\gamma$ , the NEC can be made to be satisfied here.

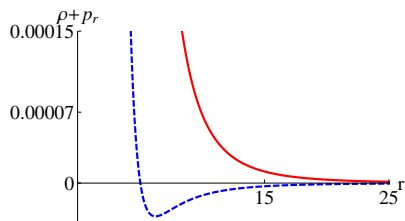


FIG. 7.  $\rho + p_r$  for the NS branch. The solid red curve is plotted with  $\gamma = 0.25$  which satisfies the NEC and the dashed blue curve for  $\gamma = 0.85$  for which the NEC is violated. Here,  $b = 1.4, c = 0.5$ .

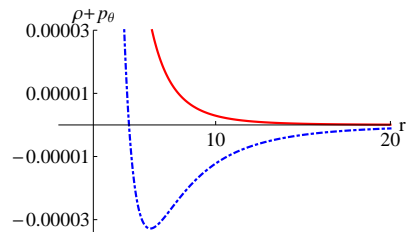


FIG. 8.  $\rho + p_\theta$  for the NS branch. The solid red curve is for  $\gamma = 0.25$  and the dashed blue curve is for  $\gamma = 0.85$ . Here,  $b = 1.4, c = 0.5$ .

### III. THE DEFORMED JMN METRIC

As a second example of using the SV method to regularise naked singularities, we now study the SV modified version of the JMN metric, which is an equilibrium end state geometry of a realistic gravitational collapse model [17]. For a specific profile of energy density and tangential pressure, the spherically symmetric JMN metric is given by

$$ds^2 = -(1 - M_0) \left( \frac{r}{r_b} \right)^{\frac{M_0}{1-M_0}} dt^2 + \frac{dr^2}{1 - M_0} + r^2 d\Omega^2. \quad (13)$$

Here  $r_b$  is a matching radius, and  $M_0$  is related to the Schwarzschild mass, to which this metric can be matched smoothly. This metric represents an unstable equilibrium configuration of a collapsing star supported by a non zero tangential pressure and vanishing radial pressure.

As discussed in [17], if we confine our attention to the parameter region  $0 < M_0 < 1$ , then the metric does not possess any event horizon, and there is a curvature singularity at  $r = 0$ . Thus, the range of the parameter  $M$ , to which we shall restrict ourselves here, is  $0 < M_0 < 1$ . It was also shown in the same work that in this geometry, there is at least one geodesic that can reach to an asymptotic observer that terminates at the singularity in the past, which points to the fact that the metric given in Eq. (13) is in fact a naked singularity. Our motivation in this section would be to check that whether this central singularity can be removed by the SV modification, and study the resulting geometry. To this end, we first write down the resulting metric using the procedure of [10], which is

given by,

$$ds^2 = -(1 - M_0) \left( \frac{\sqrt{r^2 + c^2}}{r_b} \right)^{\frac{M_0}{1-M_0}} dt^2 + \frac{dr^2}{1 - M_0} + (r^2 + c^2) d\Omega^2. \quad (14)$$

Here as usual,  $c$  is a real positive quantity. The range of the radial coordinate is  $r = -\infty$  to  $r = \infty$ , and the range of other coordinates remain same. We shall call this metric the SV-JMN solution. Now a little inspection shows that this metric actually is a traversable wormhole with a throat at  $r = 0$  for all values of the parameter  $c$ . To see this, we first note that, as mentioned before, for  $M_0 < 1$ , the metric does not possess an event horizon. Secondly, the ‘flaring out’ condition of a traversable wormhole can be checked from considering the area of the two sphere  $A(r) = (r^2 + c^2)$ , which should satisfy the conditions  $A'(r = r_0) = 0$ , and  $A''(r) = 2 > 0$ . Hence the throat is the position of the minimum area, and the wormhole is two way traversable. It can also be checked that the Ricci scalar  $R \sim (r^2 + c^2)^{-2}$ , which is finite everywhere including at  $r = 0$ . Thus we conclude that the geometry is indeed a wormhole.

### A. Photon motion in SV-JMN background

Now we briefly discuss the motion of massive and massless particles in the SV-JMN geometry, and compare them with those in the original JMN metric, the latter being studied in detail in [17],[28]. Using the standard formula for the motion of photons in spherically symmetric spacetimes given in Eq. (10), here we find the effective potential

$$V_{eff}(r) = (1 - M_0) \left( \frac{\sqrt{r^2 + c^2}}{r_b} \right)^{\frac{M_0}{1-M_0}} \left( \frac{C + L^2}{r^2 + c^2} \right), \quad (15)$$

and its derivative with respect to  $r$  is given by

$$V'_{eff}(r) = r \left( r^2 + c^2 \right)^{\frac{5M_0-4}{2(1-M_0)}}. \quad (16)$$

Clearly, we have only one physically relevant solution for the photon sphere, namely  $r = 0$ , which is just the location of the throat of the modified WH geometry. The corresponding effective potential looks like the standard effective potential for the wormhole metric, when the throat acts as a position of the photon sphere, which we have drawn in Fig. (3).

The components of the energy momentum tensor calculated from the metric in Eq. (14) are given by

$$\rho = \frac{M_0 r^2 + c^2 (2M_0 - 1)}{(c^2 + r^2)^2}, \quad p_r = -\frac{c^2}{(c^2 + r^2)^2}, \quad \text{and} \quad p_\theta = p_\phi = -\frac{M_0^2 r^2 + 2c^2 (M_0^2 - 3M_0 + 2)}{4(c^2 + r^2)^2 (M_0 - 1)}. \quad (17)$$

As can be seen directly from these expressions, the components are regular at  $r \rightarrow 0$  and reduces to the JMN values in the limit  $c \rightarrow 0$  (the role of negative pressure in gravitational collapse leading to naked singularities was investigated in [29]). In contrast to the original JMN spacetime, there is a non zero radial pressure here, which is always negative and vanishes at  $c \rightarrow 0$  as it should be. Since the original JMN metric represents the unstable equilibrium configuration of a gravitationally collapsing star with only the tangential components of pressure being

non zero, it will be interesting to study whether our metric also represents an equilibrium configuration of a collapsing matter cloud with non zero radial pressure as well as a tangential pressure.

To check if the energy conditions are violated, it enough in this case to check that NEC is violated for all values of the parameters. This can be readily seen from the expressions of  $\rho$  and  $p_r$  given above - since  $M_0 < 1$  the quantity  $\rho + p_r$  is always negative for sufficiently small values of  $r$ , and hence NEC is violated.

Finally, we point out that the SV-JMN metric we have constructed above is valid for all values of  $r$ , namely,  $-\infty < r < \infty$ . However, the JMN configuration was constructed to be the interior of collapsing matter distribution, matched with an exterior Schwarzschild solution of mass  $M_{sch} = M_0 r_b / 2$ , where the matching radius  $r = r_b$ . It may be worth mentioning that by redefining the constant  $r_b$  as  $\sqrt{r_b^2 + c^2}$ , the metric in Eq. (14) can be matched with an exterior SV metric of the form

$$ds^2 = - \left( 1 - \frac{M_0 \sqrt{r_b^2 + c^2}}{\sqrt{r^2 + c^2}} \right) dt^2 + \left( 1 - \frac{M_0 \sqrt{r_b^2 + c^2}}{\sqrt{r^2 + c^2}} \right)^{-1} dr^2 + (r^2 + c^2) d\Omega^2 . \quad (18)$$

Here  $M_{sv} = M_0 \sqrt{r_b^2 + c^2} / 2$  with  $M_{sv}$  being the mass appearing in the SV metric. Obviously the constant  $r_b$  appearing here is different from the one in Eq. (14), and we also note that for a given  $M_{sch} = M_{sv}$ , the values of  $r_b$  are different for JMN and SV-JMN metrics. In particular, for a given value of  $M_{sch} = M_{sv} = M$ , the SV-JMN solution has smaller matching radius than its JMN cousin. Since the metric outside is SV (rather than Schwarzschild), we expect the properties of accretion disks corresponding to this model to be different from those discussed in [17] and this might be interesting to investigate. Furthermore, it will be interesting to study the collapse of realistic matter with SV taken as the exterior to see whether SV-JMN solution discussed above arises as an equilibrium configuration. We hope to return to this problem in a future work.

#### IV. DISCUSSIONS AND OUTLOOK

In this paper, we have constructed and studied the properties of two classes of two-parameter spacetimes, following the Simpson-Visser method of regularising a singular metric. In the first set of metrics, we have found a new class of spacetimes that arise as deformations of the well known JNW naked singularity. By using the SV procedure, we arrive at a novel spacetime that interpolates between a naked singularity and a wormhole depending on the associated parameter space. While the WH nature of the original JNW metric for  $\gamma > 1$  was already known in the literature, here we have shown that the SV-JNW metric has a WH branch even for  $\gamma < 1$ . We have also studied the observational aspects of the metric in terms of the effective potential for photon motion in detail. Interestingly, whereas in the case of the original JNW metric, the allowed range of the parameter  $\gamma$  is  $0.5 \leq \gamma \leq 1$  for light rays to form a photon sphere, in the SV-JNW metric, even if  $\gamma \leq 0.5$  photons can form unstable orbits depending on the other parameters of interest, thereby making this metric very different from that of JNW.

Next, we have used the JMN metric as a starting point, which arises as an end state of collapse involving tangential pressures, and applied the SV procedure. To this end we have exemplified another class of metrics which solely represents a wormhole for arbitrarily small values of the SV parameter. We have in this paper restricted

ourselves to spherically symmetric models of black bounce spacetimes, though the rotating versions of these have also appeared in the literature [30]-[33]. It would be interesting to extend our models to include rotation, which we leave for a further study.

**Note Added :** While this draft was being finalised, the recent paper [34] appeared, which has partial overlap with the results presented in section II of this work.

- 
- [1] S. Carroll, *Spacetime and Geometry*, Pearson (2004).
  - [2] R. Penrose, *Riv. Nuovo Cim.* **1**, 252-276 (1969).
  - [3] M. Visser, *Lorentzian wormholes: From Einstein to Hawking*, AIP Press (1995).
  - [4] T. Damour, S. N. Solodhukin, *Phys. Rev. D* **76**, 024016 (2007).
  - [5] J. M. Bardeen, *Non-singular General Relativistic Gravitational Collapse*, in Proceedings of International Conference GR5 (Tbilisi, USSR, 1968), page 174.
  - [6] H. Maeda, arXiv:2107.04791 [gr-qc].
  - [7] R. Casadio, A. Giusti and J. Ovalle, *Phys. Rev. D* **105**, no.12, 124026 (2022).
  - [8] A. Simpson, M. Visser, *J. Cosmol. Astropart. Phys.* **2019** (2019) 042.
  - [9] A. Simpson, P. Martin-Moruno and M. Visser, *Class. Quant. Grav.* **36** (2019) 145007.
  - [10] E. Franzin, S. Liberati, J. Mazza, A. Simpson and M. Visser, *JCAP* **07**, 036 (2021).
  - [11] P. Bambhaniya, S. K. K. Jusufi and P. S. Joshi, *Phys. Rev. D* **105**, no.2, 023021 (2022).
  - [12] M. Guerrero, G. J. Olmo, D. Rubiera-Garcia and D. S. C. Gómez, *JCAP* **08** (2021), 036.
  - [13] M. Y. Ou, M. Y. Lai and H. Huang, *Eur. Phys. J. C* **82**, no.5, 452 (2022).
  - [14] Y. Guo and Y. G. Miao, arXiv:2112.01747 [gr-qc].
  - [15] A.I. Janis, E.T. Newman, J. Winicour, *Phys. Rev. Lett.* **20**, 878 (1968).
  - [16] K. S. Virbhadra, *Int. J. Mod. Phys. A* **12**, 4831-4836 (1997).
  - [17] P. S. Joshi, D. Malafarina, and R. Narayan, *Class. Quant. Grav.* **28** (2011) 235018.
  - [18] K. S. Virbhadra, S. Jhingan and P. S. Joshi, *Int. J. Mod. Phys. D* **6**, 357-362 (1997).
  - [19] K. K. Nandi, A. Islam and J. Evans, *Phys. Rev. D* **55**, 2497-2500 (1997).
  - [20] K. K. Nandi, Y. Z. Zhang and A. V. Zakharov, *Phys. Rev. D* **74**, 024020 (2006).
  - [21] M. S. Morris and K. S. Thorne, *Am. J. Phys.* **56**, 395-412 (1988).
  - [22] A. Simpson, arXiv:2104.14055.
  - [23] K. S. Virbhadra and C. R. Keeton, *Phys. Rev. D* **77**, 124014 (2008).
  - [24] S. Sau, I. Banerjee, S. SenGupta, *Phys. Rev. D* **102**, no.6, 064027 (2020).
  - [25] R. Shaikh, *Phys. Rev. D* **98**, 024044 (2018).
  - [26] R. Shaikh, P. Banerjee, S. Paul and T. Sarkar, *Phys. Lett. B* **789** 270 (2019).
  - [27] R. Shaikh, P. Banerjee, S. Paul and T. Sarkar, *JCAP* **07**, 028 (2019).
  - [28] R. Shaikh, P. Kocherlakota, R. Narayan, P. S. Joshi, *Mon. Not. Roy. Astron. Soc.* **482**, no.1, 52-64 (2019).
  - [29] F. I. Cooperstock, S. Jhingan, P. S. Joshi and T. P. Singh, *Class. Quant. Grav.* **14**, 2195-2201 (1997).
  - [30] J. Mazza, E. Franzin and S. Liberati, *JCAP* **04** (2021), 082.
  - [31] R. Shaikh, K. Pal, K. Pal and T. Sarkar, *Mon. Not. Roy. Astron. Soc.* **506** (2021) no.1, 1229-1236.

- [32] H. C. D. Lima, Junior., L. C. B. Crispino, P. V. P. Cunha and C. A. R. Herdeiro, Phys. Rev. D **103** (2021) no.8, 084040.
- [33] Z. Xu and M. Tang, Eur. Phys. J. C **81** (2021) no.10, 863.
- [34] K. A. Bronnikov, arXiv:2206.09227 [gr-qc].